

Effect of Ag-doping of Nanosized FeAlO System on its Structural, Surface and Catalytic Properties

Laila I. Ali*, Sahar A. El-Molla, Nabil H. Amin, Anwer A. Ebrahim and Hala R. Mahmoud

Chemistry Department, Faculty of Education, Ain Shams University, Roxy 11757, Cairo, Egypt

Abstract

The effects of Ag₂O-doping on the physicochemical, surface and catalytic properties FeAlO system with various extent of Fe₂O₃ loading have been investigated. The dopant concentration was changed between 1.5 and 4.0 mol % Ag₂O. Pure and variously doped solids were subjected to heat treatment at 400-800°C. The techniques employed for characterization of catalysts were TG/DTG, XRD, N₂-adsorption at -196°C and the catalytic decomposition of H₂O₂ at 25-40°C. The obtained results revealed that, the investigated catalysts consisted of nanosized γ-Al₂O₃ phase. The textural properties including S_{BET}, porosity and S_t were modified by Ag₂O-doping. The doping process with Ag-species improved the catalytic activity of FeAlO system. Increasing the precalcination temperature from 400 to 800°C increased the catalytic activity (k_{30°C}) of 3.5 % AgFeAlO with 1.9 fold towards H₂O₂ decomposition. Furthermore, the maximum increase in the k_{30°C} value due to doping with 3.5 mol% Ag₂O attained about 15.1 fold for the solids calcined at 800°C.

Keywords: Fe₂O₃/Al₂O₃ catalyst; Ag₂O-doping; Surface; Amorphous materials; H₂O₂ decomposition

Introduction

Supported transition metal oxides are interesting solids due to their surface acid-base properties [1] and oxidation-reduction potentials [2]. Iron oxide-based catalysts are very important catalysts in oxidation processes [3,4]. In spite of its catalytic potential and its availability α-Fe₂O₃ has low thermal stability against sintering which is accompanied by deactivation [5]. Therefore, supported metal oxide [6] usually exhibit modification in its textural, structural, and catalytic properties [7]. It is known that the activity and selectivity of a large variety of catalysts can be modified by loading on a finely divided support and doping with certain foreign oxides [8]. γ-Al₂O₃ is one of the supports commonly used in the petroleum refining, petrochemical industries [9], the oxidation-reduction reactions [10] and catalytic oxidation of methane [11] owing to its high specific surface area, porous structure, high thermal stability, perfect mechanical strength and acidity [12]. The surface acidity of γ-Al₂O₃ connected closely with the dispersion of the supported active metal oxides since the acid-base interaction between the metal oxides and the acid sites of γ-Al₂O₃ support promoted the dispersion of the metal oxides, which was favorable for increasing the catalytic activity [13,14]. γ-Al₂O₃, copper oxide, and ferric oxide are known as important components in automotive exhaust emission control and industrial catalysts [15].

Doping system containing transition metal oxides with certain foreign oxides is accompanied by significant modifications in their thermal stability, electrical, optical, magnetic, surface, and catalytic properties [16,17]. Many authors studied the effect of Ag⁺-doping on physicochemical properties of different supported transition metal oxides [17]. Doping of NiO catalyst with Ag₂O resulted in a progressive increase in its surface electric conductivity [18]. Doping La_{0.6}Ce_{0.4}CoO₃ catalyst with Ag⁺ alter its physical and chemical properties, such as the oxidation state of cobalt, the density of oxygen vacancies and the mobility of lattice oxygen. All these factors play important roles for NO decomposition [19]. The well-dispersed Ag⁺ ions in (C,S)-doped TiO₂ significantly promote the electron-hole separation and subsequently enhance its photoactivity [20,21]. Silver supported on γ-alumina catalyst is used for epoxidation of ethylene to ethylene oxide

below 300°C [22], and exhibited relatively good activity and selectivity for NO reduction to N₂ [23]. Doping Co₃O₄/Al₂O₃ and Co₃O₄/MgO with Ag₂O increases their catalytic activities in CO oxidation by O₂ [16,17]. Doping V₂O₅/Al₂O₃, NiO and CuO catalysts with silver oxide increased their activities towards decomposition of H₂O₂ [18,24,25]. Catalytic decomposition of H₂O₂ is an oxidation-reduction reaction, used as a green fuel/propellant instead of carcinogenic hydrazine in spaceflight at certain conditions [26]. Hydrogen peroxide can be used as an oxidizer on the fuel cells [27] instead of as liquid oxygen. Furthermore, H₂O₂ can be used as a suitable alternative fuel [28]. It has been used as a source of the hydroxyl radical (•OH) in the presence of UV irradiation for destruction of organic wastes [29]. Decomposition of H₂O₂ over metal oxides and their mixtures has been investigated by several investigators [18,24,25,30,31] to measure their catalytic activities towards the oxidation-reduction process [27].

In this paper, we aimed to investigate the influence of extent of Fe₂O₃ loading, Ag-doping and precalcination temperature of the Fe₂O₃/Al₂O₃ system on its physicochemical, surface and catalytic properties. The techniques employed were TG/DTG, XRD, nitrogen adsorption at -196°C and the catalytic decomposition of H₂O₂ at 25-40°C.

Material and Methods

Aluminum hydroxide sample was prepared by precipitating Al(NO₃)₃·9H₂O (1M) solution using 0.2M ammonia solution at 70°C and pH = 8. The precipitate was carefully washed with bi-distilled water till free from ammonium and nitrate ions, then filtered and dried at

*Corresponding author: Laila I. Ali, Chemistry Department, Faculty of Education, Ain Shams University, Roxy 11757, Cairo, Egypt, Tel: (02012) 23184682; Fax: (02) 22581243; E-mail: lailaali944@yahoo.com

Received October 13, 2011; Accepted November 16, 2011; Published December 06, 2011

Citation: Ali LI, El-Molla SA, Amin NH, Ebrahim AA, Mahmoud HR (2011) Effect of Ag-doping of Nanosized FeAlO System on its Structural, Surface and Catalytic Properties. J Thermodyn Catal 2:108. doi:10.4172/2157-7544.1000108

Copyright: © 2011 Ali LI, et al. This is an open-access article distributed under the terms of the Creative Commons Attribution License, which permits unrestricted use, distribution, and reproduction in any medium, provided the original author and source are credited.

110°C till constant weight. Al(OH)₃ sample was calcined in air at 400, 500 and 800°C for 4h.

Five specimens of Fe₂O₃/Al₂O₃ solids were prepared by impregnation known mass of Al(OH)₃ sample with solutions containing different amounts of iron nitrate dissolved in the least amount of bi-distilled water. The obtained pastes were dried at 110°C till constant weight then calcined in air at temperatures ranged between 400 and 800°C for 4 h. The nominal compositions of the prepared solids were 0.025, 0.035, 0.045, 0.055, 0.065 Fe(NO₃)₂·9H₂O: Al(OH)₃. The iron oxide content in these specimens was 3.76, 5.19, 6.58, 7.92 and 9.23 wt %, respectively. The formula of prepared solids was abbreviated as xFeAlO.

The Ag₂O-doped 0.045 Fe₂O₃/Al₂O₃ system was prepared using known mass of Al(OH)₃ impregnated with solutions containing a fixed amount of iron nitrate and different proportions of silver nitrate. The obtained pastes were dried at 110°C till constant weight then calcined in air at temperatures ranged between 400 and 800°C for 4 h. The concentration of Fe₂O₃ (6.58 wt %) and of Ag₂O added were 1.5, 2.0, 3.0, 3.5 and 4.0 mol % which corresponding 3.08, 4.06, 5.97, 6.89 and 7.80 wt %, respectively. The formula of the prepared samples was abbreviated as γAgFeAlO. All the chemicals employed were of analytical grade supplied by BDH Company.

Characterization techniques

Thermogravimetric analysis (TGA) and differential thermogravimetric analysis (DTG) of the catalysts were carried out using Shimadzu TGA-50H thermo-gravimetric analyzer; the rate of heating was kept at 10°C/min. X-ray diffractograms of various prepared solids were determined by using a Brucker diffractometer (Brucker Axs D8 Advance Germany). The Patterns were run with CuKα₁ with secondly monochromator, (λ = 0.15404 Å) at 40 kV and 40 mA at scanning rate of 2° in 2θ /min. The surface characteristics, namely specific surface areas (S_{BET}), total pore volume (V_p) and average pore radius (r̄) of the various catalysts were determined from nitrogen adsorption isotherms measured at -196°C using a Quantachrome NOVA 2000 automated gas-sorption apparatus model 7.11. All

catalysts were degassed at 200°C for 2h under a reduced pressure of 10⁻⁵ Torr before undertaking such measurements.

The catalytic activities of the various catalysts were measured by studying the decomposition of H₂O₂ at 25–40°C using 100 mg of a given catalyst sample with 0.5 ml of H₂O₂ of known concentration diluted to 20 ml with distilled water. The reaction kinetics was monitored by measuring the volume of O₂ liberated at different time intervals until no further oxygen was liberated.

Results and Discussion

Thermal properties

Thermogravimetric analysis (TGA) and differential thermogravimetric analysis (DTG) of uncalcined Al(OH)₃, 0.045FeAlO and 3.5%AgFeAlO solids were determined and shown in (Figure 1(A-C)), respectively. Inspection of Figure 1: (i) The TG curve of Al(OH)₃ solid consists of three stages. The first and second thermal processes are indicative to desorption of physisorbed water and starting the decomposition of aluminum hydroxide to aluminum oxyhydroxide Al(OOH) [32]. The last step corresponds to the complete decomposition of aluminum hydroxide into the corresponding oxide Al₂O₃. (ii) TG curve of uncalcined 0.045FeAlO solid consists of three stages. The first step represents desorption of physisorbed water and water of crystallization of iron nitrate. The second step is indicative to start the decomposition of aluminum hydroxide to aluminum oxyhydroxide compound Al(OOH) [32]. The last step corresponds to the complete decomposition of iron nitrate and aluminum oxyhydroxide into Fe₂O₃ and Al₂O₃, respectively. (iii) TG curve of uncalcined 3.5%AgFeAlO solid consists of three stages. The first step represents desorption of physisorbed water and water of crystallization of iron nitrate. The second step represents the complete decomposition of silver nitrate and aluminum hydroxide into Ag₂O and Al₂O₃, respectively. The last step corresponds to the complete decomposition of iron nitrate yielding the corresponding oxide Fe₂O₃. It can be concluded that doping Fe₂O₃/Al₂O₃ system with Ag₂O enhanced the thermal decomposition of aluminum hydroxide and ferric nitrate to Al₂O₃ and Fe₂O₃. This result

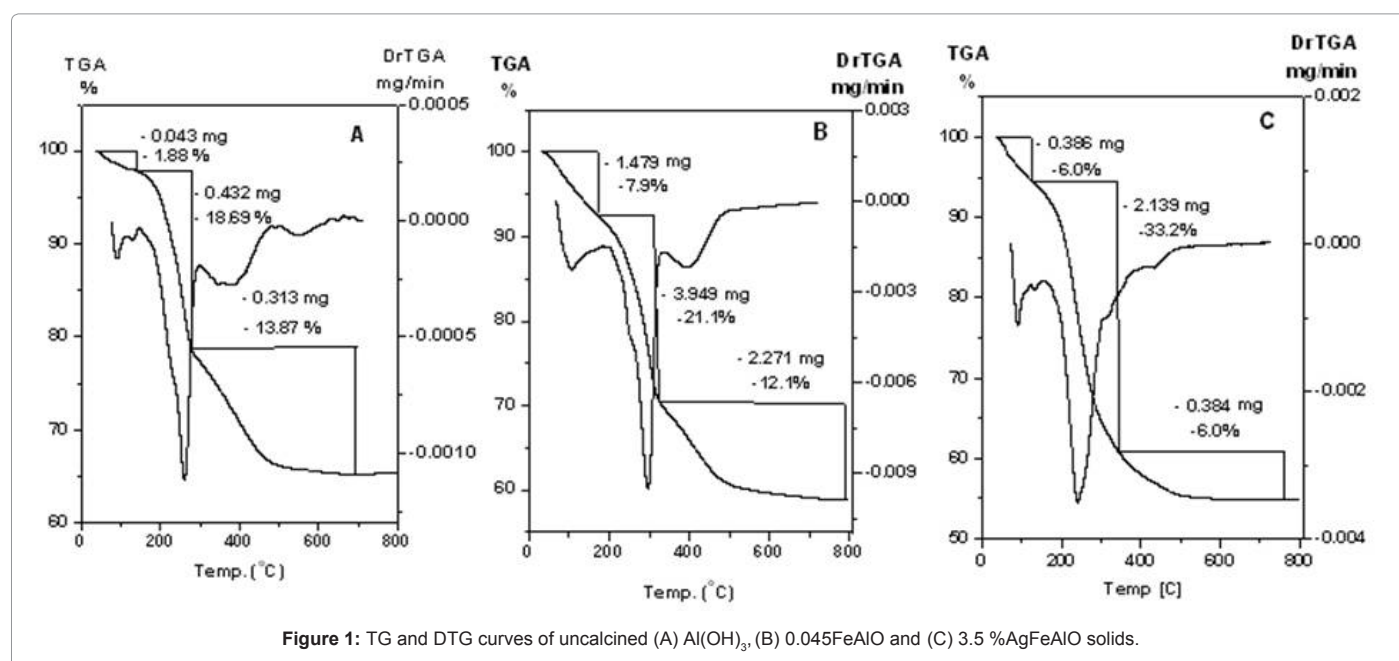


Figure 1: TG and DTG curves of uncalcined (A) Al(OH)₃, (B) 0.045FeAlO and (C) 3.5 %AgFeAlO solids.

confirmed by the previous published data [24], which indicated the presence of Ag_2O enhanced the thermal decomposition of aluminum hydroxide and ammonium vanadate to Al_2O_3 and V_2O_5 , respectively.

XRD investigation of the prepared solids

XRD of Fe_2O_3/Al_2O_3 system: The X-ray diffractograms of $\gamma-Al_2O_3$, 0.045FeAlO and 0.065FeAlO solids being calcined at 500°C were determined and illustrated in Figure 2. The effect of Fe_2O_3 loading on the degree of ordering of $\gamma-Al_2O_3$ phase was investigated as shown in Table 1. Inspection of Figure 2 and Table 1: (i) the diffractograms contain diffraction lines at d-spacing = 2.78, 2.39, 1.98 and 1.396 Å due to $\gamma-Al_2O_3$ phase which is amorphous in nature (JCPDS 10-425). There is no diffraction lines related to Fe_2O_3 phase in the investigated solids calcined at 500°C. The absence of any XRD peaks attributable to iron oxide as separate phase in Fe_2O_3/Al_2O_3 system confirms their high dispersion and its small size to be detected by XRD tool [14,24]. So, $\gamma-Al_2O_3$ acted as a convenient support for hematite. On the other hand, the crystallization temperature of pure $\alpha-Fe_2O_3$ is usually lower than 500°C, while in our samples the nucleation and growth of $\alpha-Fe_2O_3$ grains were restrained by the amorphous structure of alumina matrix [33]. (ii) Increasing the Fe_2O_3 content from 4.5 to 6.5 mol% decreases the degree of ordering of $\gamma-Al_2O_3$ phase which has nano size ≤ 6 nm.

XRD of Ag₂O-doped Fe_2O_3/Al_2O_3 system: The X-ray diffractograms of pure and Ag₂O-doped 0.045FeAlO solids being calcined at 500 and 800°C were determined and illustrated in (Figure 3A and 3B), respectively. Inspection of (Figure 3A and 3B) and (Table

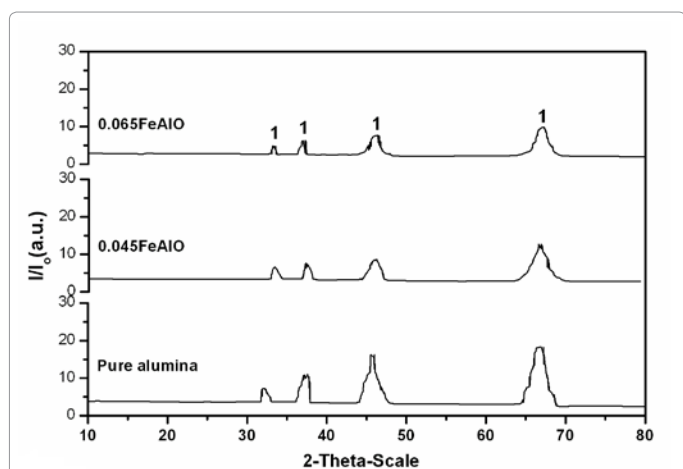


Figure 2: XRD diffractograms of pure $\gamma-Al_2O_3$ and FeAlO solids with various Fe_2O_3 loading calcined at 500°C. Lines (1) refer to $\gamma-Al_2O_3$ phase.

Solid	Calcination temperature °C	Intensity count (a.u)
		$\gamma-Al_2O_3$
Al_2O_3	500	17.1
0.045FeAlO	500	10.5
0.065FeAlO	500	8.4
Ag-0.045FeAlO %3.5	500	9.0
Al_2O_3	800	20.1
0.045FeAlO	800	14.9
Ag-0.045FeAlO %3.5	800	13.5
Ag-0.045FeAlO %4.0	800	12.5

Table 1: Intensity counts of the main diffraction lines of XRD of $\gamma-Al_2O_3$ phase for FeAlO samples calcined at 500 and 800°C.

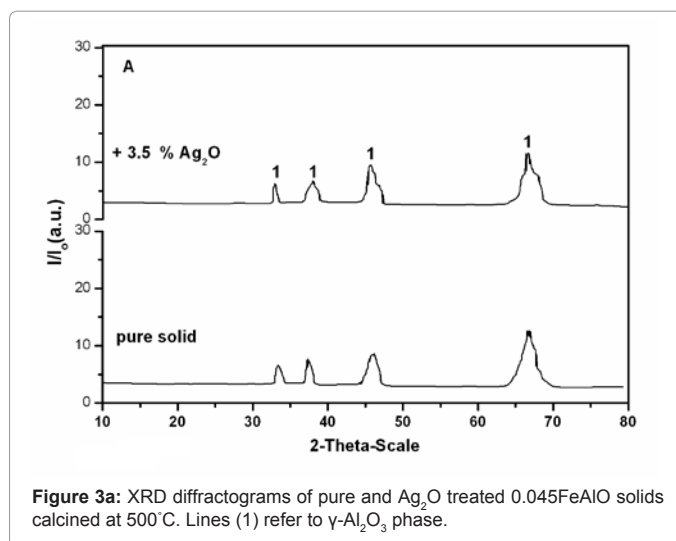


Figure 3a: XRD diffractograms of pure and Ag₂O treated 0.045FeAlO solids calcined at 500°C. Lines (1) refer to $\gamma-Al_2O_3$ phase.

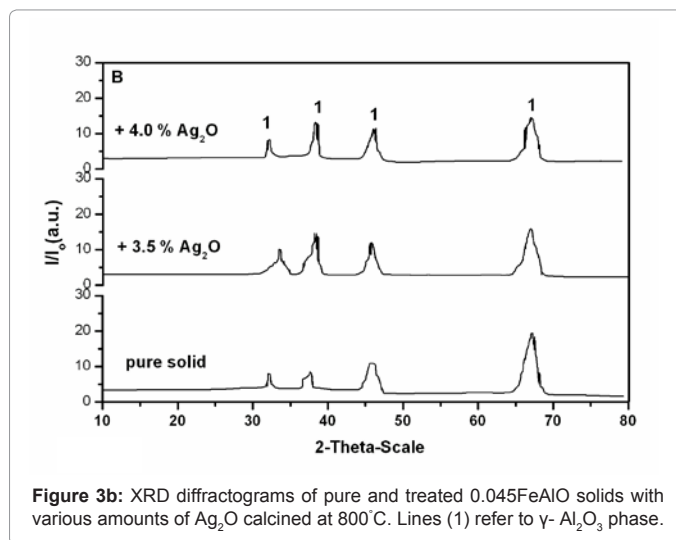


Figure 3b: XRD diffractograms of pure and treated 0.045FeAlO solids with various amounts of Ag₂O calcined at 800°C. Lines (1) refer to $\gamma-Al_2O_3$ phase.

1): (i) the diffractograms of pure and doped solids calcined at 500°C consist of diffraction peaks due to $\gamma-Al_2O_3$ phase which is amorphous in nature and there are no diffraction lines due to Fe_2O_3 phase or silver species (Ag_2O or Ag metal). (ii) The diffractograms of pure and doped solids precalcined at 800°C consist of diffraction lines related to poorly crystalline $\gamma-Al_2O_3$ phase and absence any lines related to Fe_2O_3 phase, iron aluminate spinel or silver species. (iii) Increasing the calcination temperature of pure and doped solids from 500 to 800°C increases the degree of ordering of $\gamma-Al_2O_3$ phase which has nano size (5-10 nm). (iv) Doping of 0.045FeAlO sample with Ag_2O followed by calcination at 500 and 800°C didn't much affect on the degree of ordering of $\gamma-Al_2O_3$ phase.

The above results can be explained on the light of the following: (i) absence the diffraction lines due to Ag-species (Ag_2O or Ag metal) in doped solids calcined at 500°C or 800°C was expected because of the small amounts of silver oxide added were below the detection limits of the employed X-ray diffractometer [16]. It has been reported that heating of Ag_2O at a temperature above 500°C gives metallic Ag-species [18,34] which are not detected by XRD technique because of their minute amounts. (ii) The absence of any solid-solid interaction

between Fe_2O_3 and $\gamma\text{-Al}_2\text{O}_3$ yielding aluminate spinel can be attributed to the reaction between the transition metal oxides and Al_2O_3 to produce metal aluminate is strongly dependent upon the nature of the transition metal element. The rate of reaction between the metal oxide and Al_2O_3 decreases in the following order: $\text{Cu} > \text{Co} > \text{Ni} > \text{Fe}$ [35,36]. (iii) The slight decrease in the degree of ordering of $\gamma\text{-Al}_2\text{O}_3$ phase precalcined at 500 and 800 °C due to Ag_2O -doping could be attributed to a possible coating of the $\gamma\text{-Al}_2\text{O}_3$ crystallites with Ag_2O film which hinders the particle adhesion process, thus limiting their grain growth during the course of heat treatment [37]. It has been reported that the presence of Ag effected the dispersion of Fe_2O_3 particles in the catalyst surface [38]. (iv) The increase in the degree of ordering of $\gamma\text{-Al}_2\text{O}_3$ phase for pure and doped solids due to increasing the calcination temperature from 500 to 800 °C could be explained in the light of the grain growth mechanism or sintering processes [39].

The observed changes in both of degree of ordering and crystallite sizes of $\gamma\text{-Al}_2\text{O}_3$ present in the investigated catalysts as a result of Ag_2O -doping are expected to induce changes in the specific surface areas of FeAlO system.

Surface properties

The nitrogen adsorption isotherms were measured at -196 °C for pure and Ag_2O doped samples preheated at 500 and 800 °C and illustrated in (Figure 4). The isotherms obtained are of type II of Brunauer's classification [40] showing closed hysteresis loops. The specific surface areas were calculated from these adsorption isotherms by applying the BET equation [40] the data obtained are given in (Table 2 and Figure 5A and 5B), respectively. The total pore volumes (V_p) were taken at $P/P^\circ = 0.95$ and are expressed in ml/gm. The average pore radius, \bar{r} (Å), was calculated from the above-mentioned textural properties, applying the relationship: $\bar{r} = (2V_p/S_{\text{BET}}) \times 10^4$ Å. Another series of specific surface areas S_t were computed from the V_L -t plots of the various investigated adsorbents. These plots were constructed using the de Boer-t plot [41]. The computed S_t values are given also in (Table 2). Representative V_L -t plot curves of investigated samples calcined at 500 and 800 °C are shown in (Figure 6A and 6B), respectively.

Inspection of (Figure 5A and 5B) and (Table 2) show the following: (i) addition of different amounts of Fe_2O_3 (4.5& 6.5 mol %) to $\gamma\text{-Al}_2\text{O}_3$

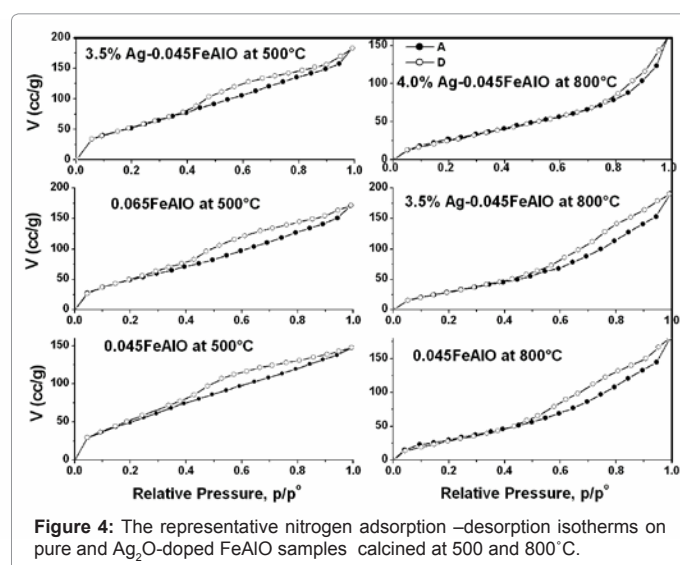


Figure 4: The representative nitrogen adsorption –desorption isotherms on pure and Ag_2O -doped FeAlO samples calcined at 500 and 800 °C.

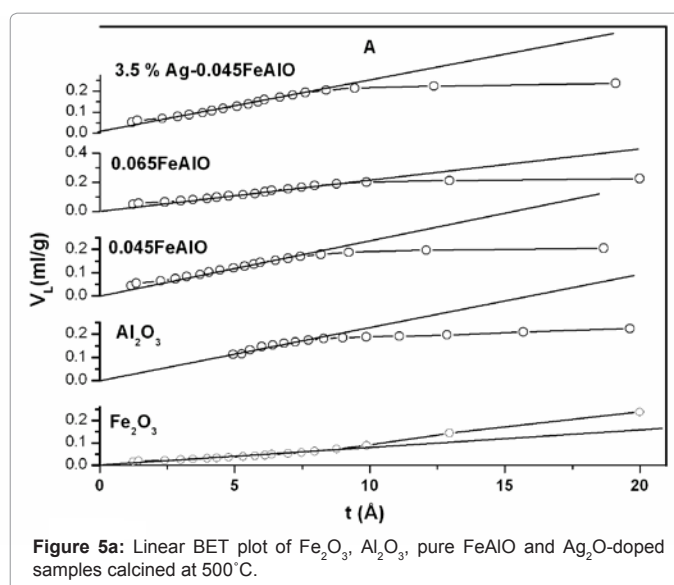


Figure 5a: Linear BET plot of Fe_2O_3 , Al_2O_3 , pure FeAlO and Ag_2O -doped samples calcined at 500 °C.

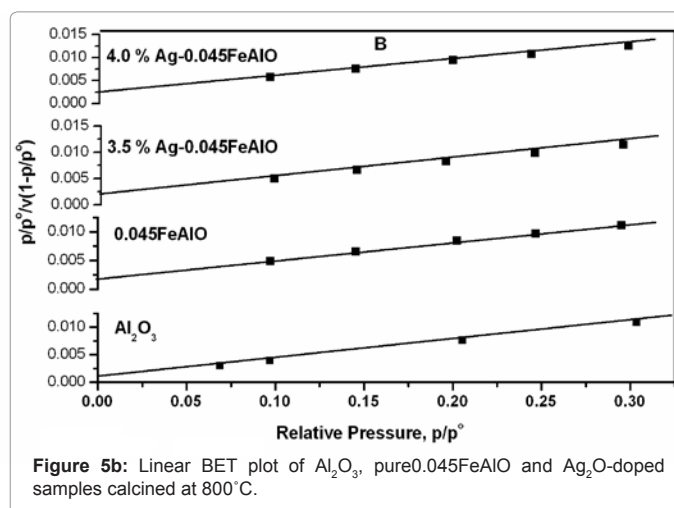


Figure 5b: Linear BET plot of Al_2O_3 , pure 0.045FeAlO and Ag_2O -doped samples calcined at 800 °C.

support followed by calcination at 500 °C resulted in a limited decrease in S_{BET} of $\gamma\text{-Al}_2\text{O}_3$ attained about 2 and 10 %, respectively. (ii) The S_{BET} of hematite precalcined at 500 °C increased by its loading on $\gamma\text{-Al}_2\text{O}_3$ support with small amount (4.5 mol %), the increase in the S_{BET} was about 204 %. Increasing Fe_2O_3 content to 6.5 mol % is accompanied by a decrease in S_{BET} of FeAlO system with about 8 %. (iii) Doping of 0.045FeAlO sample with 3.5 mol % Ag_2O followed by calcination at 500 °C led to a slight increase in its S_{BET} with about 3 %. (iv) The average pore radius \bar{r} of the investigated samples precalcined at 500 °C decreased by loading Fe_2O_3 on $\gamma\text{-Al}_2\text{O}_3$. (v) The rise in the calcination temperature of pure $\gamma\text{-Al}_2\text{O}_3$, 0.045FeAlO and 3.5% Ag_2O -0.045FeAlO samples from 500 to 800 °C brought about a significant decrease in their specific surface areas and an increase in the average pore radius \bar{r} . The decrease in S_{BET} values, due to increasing the calcination temperature, attained about 41, 39 and 42 %, respectively. (vi) Doping of 0.045FeAlO sample with 3.5 and 4.0 mol % Ag_2O followed by calcination at 800 °C led to a slight decrease in its S_{BET} which attained about 3 and 7 %, respectively. (vii) Doping of 0.045FeAlO sample with Ag_2O followed by calcination at 500 and 800 °C didn't much affect on the values of average pore radius \bar{r} of the investigated system.

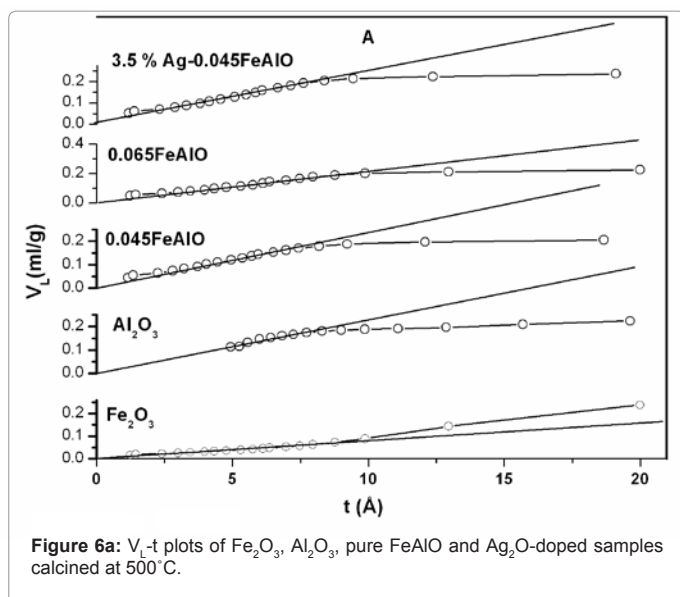


Figure 6a: V_L - t plots of Fe_2O_3 , Al_2O_3 , pure FeAlO and Ag_2O -doped samples calcined at 500°C.

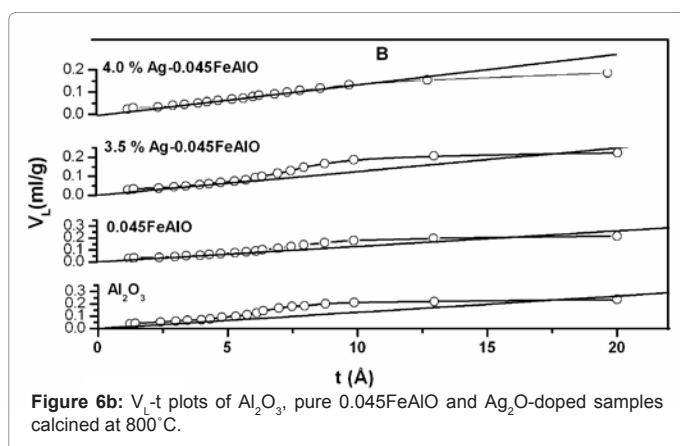


Figure 6b: V_L - t plots of Al_2O_3 , pure 0.045FeAlO and Ag_2O -doped samples calcined at 800°C.

According to V_L - t plot curves as shown in (Figure 6A and 6B) of investigated samples calcined at 500 and 800°C show the following: (i) Fe_2O_3 is mesoporous material. This behavior is indicated by the upward deviation following an initial linear region by demonstrating the existence of mesopores. (ii) The V_L - t plots of γ - Al_2O_3 , 0.045FeAlO, 0.065FeAlO, 3.5% Ag-0.045FeAlO samples calcined at 500°C and 4.0% Ag-0.045FeAlO sample calcined at 800°C reveal the microporosity character, as indicated by downward deviation from the initial straight line which passes through the origin. (iii) The V_L - t plot of γ - Al_2O_3 ,

0.045FeAlO and 3.5% Ag-0.045FeAlO samples calcined at 800°C, the initial linear region is followed by an upward deviation which is limited and a decrease in its slope is noted. This indicates the filling of some of the pores present by both multilayer formation and capillary condensation and the rest solely by multilayer formation. This indicates that these samples actually constitute of mixture of meso and micropores.

It is seen from (Table 2) that the values of S_{BET} and S_t are close to each other which justifies the correct choice of standard t -curves used in the analysis.

The changes in the specific surface areas of the prepared and calcined samples can be explained as follow: (a) the observed increase in the S_{BET} value of hematite due to loading on γ - Al_2O_3 support sample precalcined at 500°C can be discussed in the light of fine dispersion Fe_2O_3 particles on the surface of γ - Al_2O_3 [14]. Indeed, XRD peaks due to iron oxide were not detected in the investigated samples in the present work indicating that the iron oxide phase exists in a highly divided or amorphous state in these specimens. The change from the mesoporous structure to microporous structure as a result of supporting iron oxide on γ - Al_2O_3 as shown in (Figure 6A) is another factor. (b) The induced decrease in the surface area of 0.045FeAlO sample due to increasing the amount of Fe_2O_3 loading from 4.5 to 6.5 mol % may be ascribed to the aggregation of small iron species into larger bulk particles of iron in preparation process [42]. (c) The slight increase in S_{BET} value due to Ag_2O -doping precalcined at 500°C can be attributed to creation of new pores due to liberation of nitrogen oxides gases during the thermal decomposition of $AgNO_3$ dopant added [43]. (d) The observed significant decrease in S_{BET} of the investigated samples as result of increasing the calcination temperature from 500 to 800°C could be attributed to the sintering process. The sintering process might take place according to the collapse of the pore structure, pore widening [44] and/or the particle adhesion (grain growth) process together with possible phase transformation [45-47].

The observed changes in textural properties of the investigated solids as a result of increasing the extent of iron oxide loading, Ag-doping and increasing the calcination temperature should modify the concentration of catalytically active constituents taking part in the catalyzed reaction.

Catalytic properties of the prepared solids

Effect of extent of Fe_2O_3 loading on the catalytic activity of FeAlO system: Catalytic decomposition of H_2O_2 is a model reaction chosen to study the redox properties of the prepared catalysts. (Figure 7) shows the First-order plots of H_2O_2 decomposition conducted at 30°C using FeAlO catalysts at different Fe_2O_3 loading calcined at 400°C. (Figure 7)

Solid	Calcination Temperature °C	V_m (cc/g)	BET-C constants	S_{BET} (m^2/g)	S_t (m^2/g)	V_p (ml/g)	\bar{r} (Å)
Fe_2O_3	500	16.00	25.00	69.7	74.9	0.2383	68.38
Al_2O_3	500	49.72	46.35	216.4	221.2	0.2239	20.69
FeAlO	500	48.64	18.19	211.7	213.5	0.2057	19.43
0.065FeAlO	500	44.80	31.40	195.0	199.5	0.2263	23.21
Ag-0.045FeAlO%3.5	500	49.88	23.30	217.1	217.2	0.2367	21.81
Al_2O_3	800	29.38	51.43	127.9	131.7	0.2346	36.68
FeAlO	800	29.94	17.49	130.3	130.2	0.2162	33.18
Ag-0.045FeAlO %3.5	800	29.03	18.62	126.4	125.4	0.2252	35.63
Ag-0.045FeAlO %4.0	800	27.75	13.92	120.8	117.5	0.1852	30.66

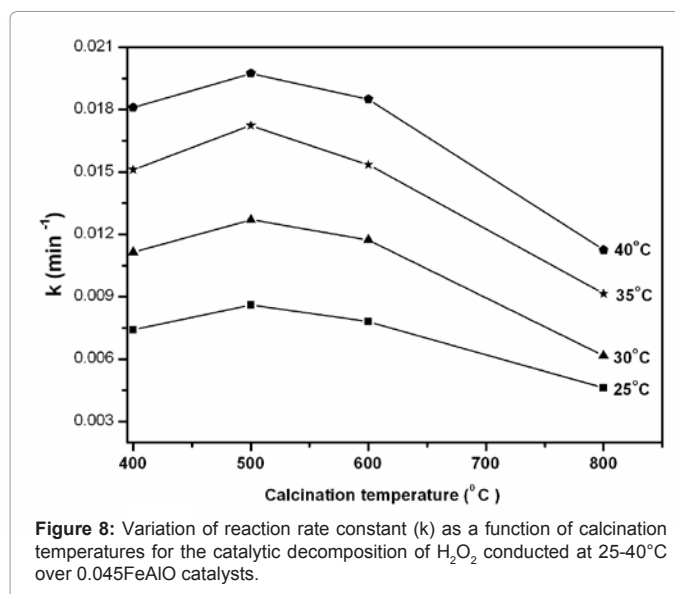
Table 2: The surface characteristics of investigated pure and doped FeAlO samples calcined at 500 and 800°C.

shows that γ - Al_2O_3 support solid exhibits no catalytic activity towards H_2O_2 decomposition reaction. The catalytic activity of FeAlO catalyst is higher than that of pure Fe_2O_3 catalyst. The increase in amount of Fe_2O_3 content from 2.5 to 6.5 mol% is accompanied by increasing the catalytic activity of FeAlO system precalcined at 400°C . The maximum increase in the catalytic activity attained about 34 % for 0.065FeAlO catalyst at $k_{30^\circ\text{C}}$ with respect to pure Fe_2O_3 .

XRD and S_{BET} measurements showed that the high dispersion of Fe_2O_3 on γ - Al_2O_3 and the significant increase in the S_{BET} may be responsible for the higher catalytic activity of FeAlO than the pure Fe_2O_3 . The absence of any XRD patterns detected for Fe_2O_3 as separate phase reflected the decrease in the crystallite size of detected phase which becomes so small to be detected by the employed XRD technique and hence increasing the surface area of investigated solids. Other factor, we cannot overlook, is the creation of bivalent catalytic centers [32,48] such as Fe^{3+} - Fe^{2+} ion pairs that are involved in H_2O_2 -decomposition reaction. It has been reported that a favorable redox couple of Fe^{2+} - Fe^{3+} is essential for catalytic decomposition of H_2O_2 through electron exchange [49].

Effect of calcination temperature on the catalytic activity of 0.045FeAlO system: Variation of the catalytic activity expressed as reaction rate constant ($k \text{ min}^{-1}$) as a function of precalcination temperature of 0.045FeAlO system in the range of 400 - 800°C towards H_2O_2 decomposition conducted at 25 - 40°C was investigated and determined as shown in (Figure 8). Inspection of (Figure 8) (i) Increasing the calcination temperature from 400 to 500°C increases the catalytic activity of 0.045FeAlO system; the increase in the $k_{30^\circ\text{C}}$ value attained about 14 %. (ii) Increasing the calcination temperature from 500 to 800°C was accompanied by a progressive decrease in the catalytic activity of 0.045FeAlO system; the decrease in the $k_{30^\circ\text{C}}$ value attained about 45 %. (iii) The catalytic activity of 0.045FeAlO system increased with increasing the reaction temperature from 25 to 40°C .

Increasing the catalytic activity of 0.045FeAlO system as a result of increasing the calcination temperature from 400 to 500°C may be attributed to increase in the concentration of catalytically active constituents of Fe^{3+} - Fe^{2+} ion pairs taking part in the catalysis of H_2O_2 -



decomposition reaction. The progressive decrease in the catalytic activity of 0.045FeAlO system as a result of increasing the calcination temperature from 500 to 800°C may be due to (i) increasing the degree of ordering of γ - Al_2O_3 phase (Table1). (ii) The sintering process of catalytically active sites with subsequent decrease in its specific surface area from 211.7 to $130.3 \text{ m}^2 \text{ g}^{-1}$ (Table 2) [50,51]. (iii) The effective removal of surface OH groups which act as active sites for the H_2O_2 decomposition reaction [37].

Effect of Ag_2O -doping on the catalytic activity of 0.045FeAlO system calcined at different calcination temperatures: Variation of the catalytic activity expressed as reaction rate constant ($k \text{ min}^{-1}$) of H_2O_2 decomposition conducted at 25 - 40°C as a function of wt % of Ag_2O for the solids precalcined at 500 and 800°C was investigated and graphically represented in (Figure 9A and 9B), respectively. The variation of $k \text{ (min}^{-1}\text{)}$ of H_2O_2 decomposition over 3.5 % AgFeAlO conducted at 30°C as a function of calcination temperature is graphically represented in (Figure 10). It is seen from these (Figures 9 and 10) that: (i) the catalytic activity of 0.045FeAlO catalysts increases progressively by increasing the amounts of dopant up to certain extent reaching to a maximum at 3.5 mol % Ag_2O , the increase in the $k_{30^\circ\text{C}}$ value of 3.5 % AgFeAlO calcined at 500°C attained about 502 %. (ii) Increasing Ag_2O content to 4.0 mol % is accompanied by a sharp decrease in the catalytic activity falling to values greater than that of pure catalysts precalcined at the same temperature. The maximum decrease in the $k_{30^\circ\text{C}}$ value on increasing the amount of dopant from 3.5 to 4.0 mol % attained about 40 and 30 % for the catalysts precalcined at 500 and 800°C , respectively. (iii) The catalytic activity of pure and doped 0.045FeAlO system increased with increasing the reaction temperature from 25 to 40°C . (iv) The catalytic activity of doped 0.045FeAlO solid with 3.5 mol % Ag_2O increases progressively by increasing the calcination temperature from 400 to 800°C . The increase in the $k_{30^\circ\text{C}}$ value due to doping with 3.5 mol % Ag_2O attained about 383, 502, 635 and 1511 % for the catalysts precalcined at 400 , 500 , 600 and 800°C , respectively.

The significant enhancement in the catalytic activity of 0.045FeAlO solids in the investigated redox reaction as a result of Ag_2O -doping could be discussed in terms of: (i) the slight decrease in the degree of ordering of γ - Al_2O_3 phase in 3.5 % AgFeAlO sample calcined at 500°C

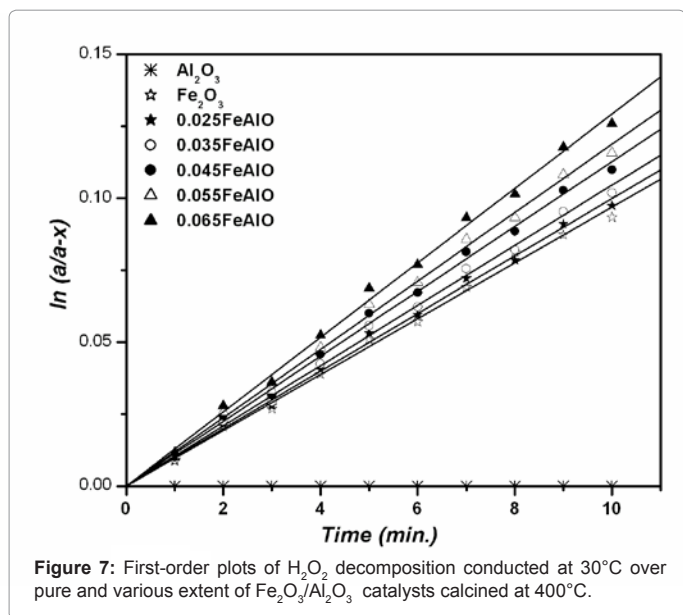


Figure 7: First-order plots of H_2O_2 decomposition conducted at 30°C over pure and various extent of $\text{Fe}_2\text{O}_3/\text{Al}_2\text{O}_3$ catalysts calcined at 400°C .

(as shown in XRD section). This effect could result from a possible coating of the γ -Al₂O₃ support with an Ag₂O film which acts as an energy barrier opposing their particles adhesion. This reflected the role of Ag₂O treatment in increasing the degree of dispersion of Fe₂O₃ and consequently increasing the catalytic activity of H₂O₂ decomposition. (ii) The possible changes in the concentration of ion pairs acting as active sites for the catalyzed reaction present in the outermost surface layers of the treated solids [24,52,53]. The created ion pairs due to Ag₂O-doping may be Ag⁺-Fe²⁺, Ag-Fe³⁺ and Ag-Ag⁺ [25].

However, the observed significant decrease in the $k_{30^\circ\text{C}}$ value on increasing the amount of dopant from 3.5 to 4.0 mol% can be attributed to decrease in the concentration of catalytically active species involved in the catalyzed reaction. This could result from the location of dopant species on the surface layers of the treated catalysts thus blocking some of the active constituents by dopant cation and/or metallic silver [54].

The observed increase in the catalytic activity of Ag-doped FeAlO

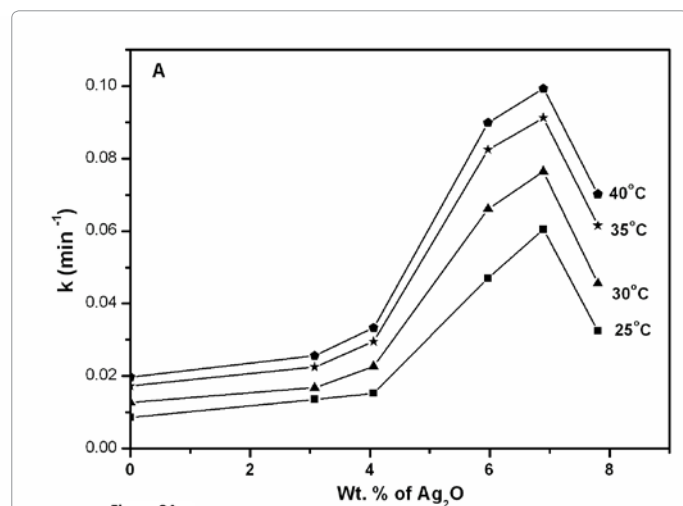


Figure 9a: Variation of reaction rate constant (k) as a function of wt % of Ag₂O for the catalytic decomposition of H₂O₂ conducted at 25-40°C over pure 0.045FeAlO catalysts calcined at 500°C.

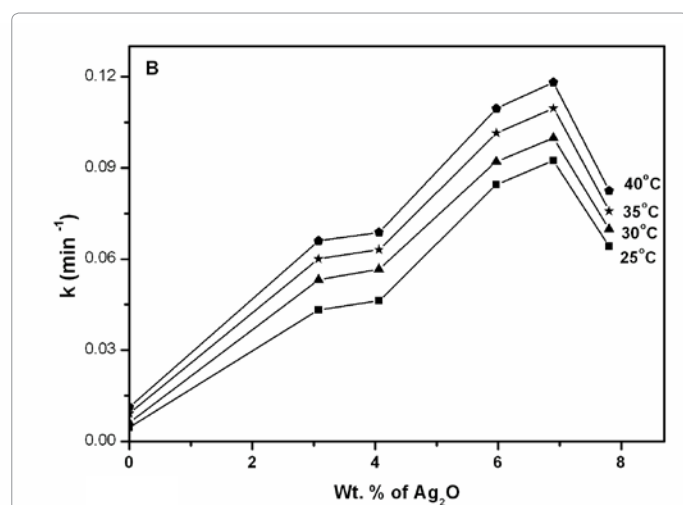


Figure 9b: Variation of reaction rate constant (k) as a function of wt % of Ag₂O for the catalytic decomposition of H₂O₂ conducted at 25-40°C over pure 0.045FeAlO catalysts calcined at 800°C.

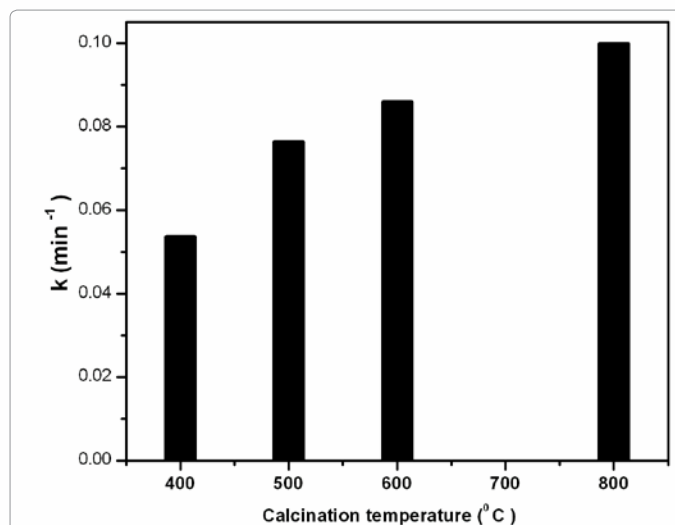


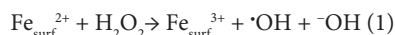
Figure 10: Variation of reaction rate constant (k) as a function of calcination temperatures for the catalytic decomposition of H₂O₂ conducted at 30°C over 3.5%AgFeAlO catalysts.

solids by increasing the calcination temperature from 400 to 800°C (Figure 10) could be attributed to the possible presence of metallic Ag-species and increase in the concentration of surface excess oxygen as a result of heating at a temperature above 450°C [18,34] according to the following reaction [55].

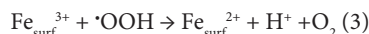


In spite of increasing the calcination temperature decreases the surface areas of the Ag-doped solid catalysts. The observed increase in catalytic activity clearly reflects the minor role played by surface area in determining the catalytic activity of doped solids.

The formation of radicals from H₂O₂ and iron oxides has been proposed in the literature [56]. The mechanism of catalytic decomposition of H₂O₂ by radicals generation could be explained by the possible initiation the reaction with partially reduced surface specie, for example, Fe²⁺, according to the Haber-Weiss mechanism:



The formation of O₂ in a radical reaction can be very complex but a simple pathway can be proposed via the hydroperoxide radical:



In these reactions a hydroperoxide radical intermediate is generated, which can then react with a surface species to produce O₂ and H⁺. The H⁺ is then neutralized by the OH⁻ generated in (Equation 1).

The present Fe³⁺ for the solids calcined at 800°C is reduced during the decomposition of hydrogen peroxide (as shown in Equation 3) there is the possibility to regenerate the Fe²⁺, which can catalyze the decomposition process [57].

Conclusions

Doping with Ag₂O enhanced the thermal decomposition of aluminum hydroxide and ferric nitrate to Al₂O₃ and Fe₂O₃. Ag₂O-doping led to a slight decrease in the degree of ordering of γ -Al₂O₃ phase

precalcined at 500 and 800°C. Doping of 0.045FeAlO catalyst with 3.5 or 4.0 mol % Ag₂O preheated at 800°C decreased its BET-surface area. The catalytic activity of FeAlO system towards H₂O₂ decomposition increased by increasing the Fe₂O₃ content and Ag₂O amount up to 3.5 mol%. The maximum increase in the catalytic activity attained about 34 % for 0.065FeAlO catalyst at k_{30°C} with respect to un-supported Fe₂O₃. The maximum increase in the catalytic activity measured at k_{30°C} due to 3.5 mol % Ag₂O-doping attained about 15.1 fold for the solids calcined at 800°C.

References

1. Khaleel A, Shehadi I, Shamisi M (2010) Nanostructured chromium-iron mixed oxides: Physicochemical properties and catalytic activity. *Colloids Surf A* 355: 75-82.
2. Cao JL, Wang Y, Yu XL, Wang SR, Wu SH et al. (2008) Mesoporous CuO-Fe₂O₃ composite catalysts for low-temperature carbon monoxide oxidation. *Appl Catal B* 79: 26-34.
3. Al-Sayari S, Carley AF, Taylor SH, Hutchings GJ (2007) Au/ZnO and Au/Fe₂O₃ catalysts for CO oxidation at ambient temperature: comments on the effect of synthesis conditions on the preparation of high activity catalyst prepared by coprecipitation. *Top Catal* 44: 123-128.
4. Wang HC, Chang SH, Hung PC, Hwang JF, Chang MB (2008) Catalytic oxidation of gaseous PCDD/Fs with ozone over iron oxide catalysts. *Chemosphere* 71: 388-397.
5. Liu XH, Shen K, Wang YG, Wang YQ, Guo YL et al. (2008) Preparation and catalytic properties of Pt supported Fe-Cr mixed oxide catalysts in the aqueous-phase reforming of ethylene glycol. *Catal Commun* 9: 2316-2318.
6. Klabunde KJ, Khaleel A, Park D (1995) Overlayer of iron oxide on nanoscale magnesium oxide crystallites: chlorocarbon destruction by catalytic solid-state ion/ion exchange. *High Temp Mater Sci* 33: 99-106.
7. Wachs I.E (2005) Recent conceptual advances in the catalysis science of mixed metal oxide catalytic Materials. *Catal Today* 100: 79-94.
8. El-Molla SA (2006) Dehydrogenation and condensation in catalytic conversion of iso-propanol over CuO/MgO system doped with Li₂O and ZrO₂. *Appl Catal A* 298:103-108.
9. Jun Cheng L, Lan X, Feng X, Wen WZ, Fei W (2006) Effect of hydrothermal treatment on the acidity distribution of γ-Al₂O₃ support. *Appl Surf Sci* 253: 766-770.
10. El-Shobaky GA, El-Khouly SM, Ghozza AM, Mohamed GM (2006) Surface and catalytic investigations of CuO-Cr₂O₃/Al₂O₃ system. *Appl Catal A* 302: 296-304.
11. Lippits MJ, Boer Iwema RRH, Nieuwenhuys BE (2009) A comparative study of oxidation of methanol on γ-Al₂O₃ supported group IB metal catalysts. *Catal Today* 145: 27-33.
12. Stiles AB (1987) "Catalyst Supports and Supported Catalysts: Theoretical and Applied Concepts", Butterworths, Boston.
13. Uguina MA, Delgado JA, Rodríguez A, Carretero J, Gómez-Díaz D (2006) Alumina as heterogeneous catalyst for the regioselective epoxidation of terpenic diolefins with hydrogenperoxide. *J Mol Catal A* 256: 208-215.
14. Wu Y, Gao F, Liu B, Dai Y, Zhu H, et al. (2010) Influence of ferric oxide modification on the properties of copper oxide supported on γ- alumina. *J Colloid Interface Sci* 343: 522-528.
15. Ozawa M, Suzuki S, Loong CK, Richardson JW, Thomas RR (1997) Structural phase transitions and lean NO removal activity of copper-modified Alumina. *Appl Surf Sci* 121-122: 441-444.
16. El-Shobaky GA, Shouman MA, El-Khouly SM (2003) Effect of silver oxide doping on surface and catalytic properties of Co₃O₄/Al₂O₃ system. *Mater Lett* 58:184-190.
17. Deraz NM (2001) Effect of Ag₂O doping on surface and catalytic properties of cobalt-magnesia Catalysts. *Mater Lett* 51: 470-477.
18. Turkey AM (2003) Electrical surface and catalytic properties of NiO as influenced by doping with CuO and Ag₂O. *Appl Catal A* 247: 83-93.
19. Liu Z, Hao J, Fu L, Zhu T (2003) Study of Ag/La_{0.8}Ce_{0.4}CoO₃ catalysts for direct decomposition and reduction of nitrogen oxides with propene in the presence of oxygen. *Appl Catal B* 44: 355-370.
20. Hamal DB, Klabunde KJ (2007) Synthesis, characterization, and visible light activity of new nanoparticle photocatalysts based on silver, carbon, and sulfur-doped TiO₂. *J Colloid Interface Sci* 311: 514-522.
21. Zielińska-Jurek A, Kowalska E, Sobczak JW, Lisowski W, Ohtani B, et al. (2011) Preparation and characterization of monometallic (Au) and bimetallic (Ag/Au) modified-titania photocatalysts activated by visible light. *Appl Catal B* 101: 504-514.
22. Wu Y, Yan A, He Y, Wu B, Wu T (2010) Ni-Ag-O as catalyst for a novel one-step reaction to convert ethane to ethylene oxide. *Catal Today* 158:258-262.
23. She X, Flytzani-Stephanopoulos M (2006) The role of Ag-O-Al species in silver-alumina catalysts for the selective catalytic reduction of NO_x with methane. *J Catal* 237:79-93.
24. Shaheen WM (2006) Thermal solid-solid interactions and catalytic properties of V₂O₅/Al₂O₃ system treated with Li₂O and Ag₂O. *Mater Sci Eng B* 135: 30-37.
25. Turkey A M, Radwan N R E, El-Shobaky G A (2001) Surface and catalytic properties of CuO doped with MgO and Ag₂O. *Colloids Surf A* 181: 57-68.
26. Teshimal N, Genfa Z, Dasgupta P K (2004) Catalytic decomposition of hydrogen peroxide by a flow-through self-regulating platinum black heater. *Anal Chim Acta* 510: 9-13.
27. Sanli A E, Aytan A (2011) Response to Disselkamp: Direct peroxide/peroxide fuel cell as a novel type fuel cell. *Int Hydrogen Energy* 36: 869-875.
28. Wee J-H (2006) Which type of fuel cell is more competitive for portable application: direct methanol fuel cells or direct borohydride fuel cells?. *J Power Sources* 161:1-10.
29. Bandara J, Mielczarski J A, Lopez, Kiwi J (2001) Sensitized degradation of chlorophenols on iron oxides induced by visible light. Comparison with titanium oxide. *Appl Catal B* 34: 321-333.
30. Rao G R, Sahu H R, Mishra B G (2003) Surface and catalytic properties of Cu-Ce-O composite oxides prepared by combustion method. *Colloids Surf A* 220: 261-269.
31. Renuka NK (2010) A green approach for phenol synthesis over Fe³⁺/MgO catalysts using hydrogen peroxide. *J Mol Catal A* 316:126-130.
32. Shaheen W M, Hong K S (2002) Thermal characterization and physicochemical properties of Fe₂O₃-Mn₂O₃/Al₂O₃ system. *Thermochim Acta* 381:153-164.
33. Liu M, Lib H, Xiao L, Yu W, Lu Y, Zhao Z (2005) XRD and Mössbauer spectroscopy investigation of Fe₂O₃-Al₂O₃ nano-composite. *J Magn Magn Mater* 294: 294-297.
34. Imamura S, Yamada H, Utani K (2000) Combustion activity of Ag/CeO₂ composite catalyst. *Appl Catal A* 192: 221-226.
35. Gardener S D, Hoflund G B, Upchurch B T, Schryer D R, Kielin E J, Schryer J (1991) Comparison of the performance characteristics of Pt/SnO₂ and Au/MnO_x catalysts for low-temperature CO oxidation. *J Catal* 129: 114-120.
36. Fagal GA, El-Shobaky GA, El-Khouly SM (2001) Surface and catalytic properties of Fe₂O₃-Cr₂O₃/Al₂O₃ solids as being influenced by Li₂O and K₂O-doping. *Colloids Surf A* 178: 287-296.
37. El-Shobaky G A, Amin N H, Deraz N M, El-Molla, S A (2001) Decomposition of H₂O₂ on pure and ZnO-treated Co₃O₄/Al₂O₃ solids. *Adsorp Sci Technol* 19 (1): 45-58.
38. Brinen JS, Schmitt JL, Doughman WR, Achorn PJ, Siegel LA et al.(1975) X-ray photoelectron spectroscopy studies of the rhodium on charcoal catalyst: II. Dispersion as a function of reduction. *J Catal* 40: 295- 300.
39. Shaheen WM (2007) Thermal behaviour of pure and binary Fe(NO₃)₃·9H₂O and (NH₄)₆Mo₇O₂₄·4H₂O systems. *Mater Sci Eng A* 445-446:113-121.
40. Brunauer S, Emmett PH, Teller E (1938) Adsorption of Gases in Multimolecular Layers. *J Am Chem Soc* 60: 309-319.

41. Lippens BC, deBoer JH (1965) Studies on pore systems in catalysts: V. The t method. *J Catal* 4: 319-323.
42. Wang JB, Lin SC, Huang TJ (2002) Selective CO oxidation in rich hydrogen over CuO/samarium-doped ceria. *Appl Catal A* 232:107-120.
43. El-Molla SA, Hammed MN, El-Shobaky G A (2004) Catalytic conversion of isopropanol over NiO/MgO system doped with Li₂O. *Mater Lett* 58: 1003-1011.
44. El-Shobaky GA, Deraz NM (2001) Surface and catalytic properties of cobaltic oxide supported on an active magnesia. *Mater Lett* 47: 231-240.
45. Deraz NM (2008) Production and characterization of pure and doped copper ferrite nanoparticles. *J Anal Appl Pyrolysis* 82:212-222.
46. Deraz NM (2003) The formation and physicochemical characterization of Al₂O₃-doped manganese ferrites. *Thermochim Acta* 401:175-185.
47. Radwan NRE, El-Sharkawy EA, Youssef AM (2005) Influence of gold and manganese as promoters on surface and catalytic performance of Fe₂O₃/Al₂O₃ system. *Appl Catal A* 28: 93-106.
48. Mucka V, Tabacik S (1991) Catalytic properties of nickel-cobalt mixed oxides and the influence of ionizing radiation. *Radiat Phys Chem* 38: 285 -290.
49. Parida KM, Dash SS, Mallik S, Das J (2005) Effect of heat treatment on the physico-chemical properties and catalytic activity of manganese nodules leached residue towards decomposition of hydrogen peroxide. *J Colloid Interface Sci* 290: 431- 436.
50. Shaheen WM (2002) Thermal solid-solid interaction and catalytic properties of CuO/Al₂O₃ system treated with ZnO and MoO₃. *Thermochim Acta* 385: 105-116.
51. Shaheen WM (2007) Effects of thermal treatment and doping with cobalt and manganese oxides on surface and catalytic properties of ferric oxide. *Mater Chem Phys* 101:182-190.
52. Shaheen WM, Ali AA (2001) Thermal solid-solid interaction and physico-chemical properties of CuO-Fe₂O₃ system. *Int J Inorg Mater* 3: 1073-1081.
53. Shaheen WM, Zahran AA, El-Shobaky GA (2003) Surface and catalytic properties of NiO/MgO system doped with Fe₂O₃. *Colloids Surf A* 231: 51-65.
54. Radwan NRE, Turky AM, El-Shobaky GA (2002) Surface and catalytic properties of CuO doped with Li₂O and Al₂O₃. *Colloids Surf A* 203: 205-215.
55. Anand S, Srivastava ON (2002) Effect of AgNO₃ additive/doping on microstructure and superconductivity of the Pb doped Hg: 1223 thin film prepared through spray pyrolysis. *J Phys Chem Solids* 63:1647-1653.
56. Kwan WP, Voelker BM (2003) Rates of hydroxyl radical generation and organic compound oxidation in mineral-catalyzed Fenton-like systems. *Environ Sci Technol* 37: 1150-1158.57.
57. Costa RCC, Lelis MFF, Oliveira LCA, Fabris JD, Ardisson JD et al. (2006) Novel active heterogeneous Fenton system based on Fe_{3-x}M_xO₄ (Fe, Co, Mn, Ni): The role of M²⁺ species on the reactivity towards H₂O₂ reactions. *J Hazard Mater B* 129:171-17.